hemato

MDPI

Article

Role of ^{18}F-FDG PET/CT in the Management of Patients Affected by HHV-8-Associated Multicentric Castleman's Disease

Domenico Albano *, Francesco Bertagna, Elisabetta Cerudelli, Francesco Dondi and Raffaele Giubbini

Nuclear Medicine, University of Brescia and ASST Spedali Civili Brescia, 25123 Brescia, Italy; frabcescobertagna@unibs.it (F.B.); elisabetta.cerudelli@gmail.com (E.C.); f.dondi@outlook.it (F.D.); raffaele.giubbini@unibs.it (R.G.)

* Correspondence: domenico.albano@unibs.it

Abstract: Our aim was to investigate the usefulness of 18fluorine-fluorodeoxyglucose positron emission tomography/computed tomography (^{18}F-FDG PET/CT) in the diagnosis, treatment response evaluation, and follow-up of human herpesvirus-8 (HHV-8)-associated multicentric Castleman's disease (MCD). Fifteen patients with histologically diagnosis of HHV-8-associated MCD were retrospectively included. For all patients, a ^{18}F-FDG PET/CT scan was performed before any treatment for diagnosis and PET/CT scans after Rituximab (4 cycles) for the evaluation of treatment response; moreover, 22 PET/CT were performed during the follow-up to check disease status. To evaluate treatment response, we applied Deauville criteria. PET/CT findings were compared with other conventional imaging (CI) findings. At diagnosis, ^{18}F-FDG PET/CT showed an increased FDG-uptake in all cases corresponding to lymph nodes and confirming the MCD. The average SUVmax of the FDG avid lesions were 8.75, average lesion-to-liver SUVmax ratio was 3.6, and average lesion-to-blood pool SUVmax ratio was 3.9. After first-line therapy, ^{18}F-FDG PET/CT resulted negative (Deauville score < 4) in seven patients and positive in the remaining eight (Deauville score 4–5). A negative restaging PET/CT was associated with a lower risk of relapse. During follow-up, PET/CT detected the presence of relapse or progression in 5 (23%) cases with an accuracy higher than CI. ^{18}F-FDG PET/CT seems to be an useful tool in studying HHV-8-associated MCD both at diagnosis and during follow-up.

Keywords: Castleman disease; MCD; ^{18}F-FDG; PET/CT; HHV-8

Citation: Albano, D.; Bertagna, F.; Cerudelli, E.; Dondi, F.; Giubbini, R. Role of ^{18}F-FDG PET/CT in the Management of Patients Affected by HHV-8-Associated Multicentric Castleman's Disease. *Hemato* **2021**, *2*, 383–391. https://doi.org/10.3390/hemato2020024

Academic Editor: Alberto Signore

Received: 17 May 2021
Accepted: 18 June 2021
Published: 20 June 2021

1. Introduction

Castleman disease (CD) includes a group of rare hematologic diseases characterized by the presence of lymphoadenopathies with peculiar histopathology and associated with biochemical and clinical abnormalities. CD may be classified as unicentric (UCD) and multicentric (MCD) according to the number and sites of disease and may be further divided based on etiological nature into human herpesvirus-8-associated (HHV8-associated) MCD, POEMS-associated MCD, and idiopathic MCD [1–4]. The diagnostic evaluation of MCD has a crucial role in the management of patients affected by this disease; it is very important to detect whether CD is limited to one site or also affects other nodes [4]. At diagnosis, a comprehensive clinical evaluation, including laboratory tests (like blood counts, markers inflammation, serum cytokine levels, viral serology for HHV-8 and HIV, protein electrophoresis, and quantitative immunoglobulins), is recommended but the histological confirmation derived usually by lymph node biopsy [5]. Currently, computed tomography (CT) is routinely utilized in CD patients with the aim to identify and describe lymph nodes by shape, size, and contrast-enhancement pattern [6]. Usually, lymph nodes have an increased and rapid contrast enhancement on CT. However, CT presents several limitations, such as the difficulties in discriminating between reactive/inflammatory and pathological nodes and between inactive and active disease status. Moreover, after treatment, the lymph

nodes may remain present for a long period despite a metabolic/functional response. The effective role of 18fluorine-fluorodeoxyglucose positron emission tomography/CT (^{18}F-FDG PET/CT) in studying CD is yet unclear, with promising and initial evidences in small number case series and heterogeneous population (different CD forms included) [7–11]. Specific papers about HHV-8-associated MCD are lacking. As demonstrated in other diseases, the metabolic-functional response may precede anatomical/morphological response and help to better stratify the patients.

Consequently, the aim of our study was to investigate the usefulness of ^{18}F-FDG PET/CT in the diagnosis, treatment response evaluation, and follow-up of HHV-8-associated MCD.

2. Materials and Methods

From January 2015 and December 2020, we retrospectively included 15 patients (10 men; 5 women) with an average age of 51 years (range 14–79) and a histological diagnosis of HHV-8-associated MCD who underwent ^{18}F-FDG PET/CT during the course of disease. The main features of our population are displayed in Table 1. Clinical and pathologic factors such as age, gender, presence of symptoms (fever), histologic subtypes, immune system status, and the main laboratory findings (hemoglobin, platelet, albumin, LDH, and C-reactive protein (CRP) levels) near to the baseline PET/CT were obtained from medical data. In all, they underwent 52 ^{18}F-FDG PET/CT scans: 15 for initial diagnosis of MCD, 15 for the evaluation of treatment response after first-line therapy, and 22 during follow-up for restaging purposes. As first-line therapy, all patients received four cycles of Rituximab (375 mg/m^2), and ^{18}F-FDG PET/CT scans were done at least 3 weeks after the last Rituximab administration. The median follow-up of our population was 36 months (range 12–66).

Table 1. Baseline characteristics of 15 patients.

	N° (%)
Age average (range)	51 (14–79)
Gender male	10 (67%)
female	5 (33%)
Size lymph node cm average (range)	2.8 (1.1–5.5)
HIV positive	4 (27%)
Fever	7 (47%)
Histologic subtype: Hyaline vascular	7 (47%)
Plasma cell	5 (33%)
Mixed	3 (20%)
Hemoglobin low * (NR 130–180 man; 115–160 woman) (g/L)	4 (27%)
Hemoglobin g/L average (range)	119 (95–140)
Platelet low * 10^9/L (NR 150–450)	4 (27%)
Platelet 10^9/L average (range)	140 (100–320)
Albumin low * (g/L) (NR 4–5.4)	5 (33%)
Albumin g/L average (range)	4.5 (3.5–5.4)
Leucocyte count low * (NR 4–11) 10^9/L	5 (33%)

Table 1. *Conts.*

	N° (%)
Leucocyte 10^9/L average (range)	4 (2.9–8)
CRP > 0.4 mg/L	11 (73%)
Average (range)	5.7 (0.2–99)
LDH > 115 IU/L	6 (40%)
LDH IU/L average (range)	113 (102–250)
N° PET/CT	52
PET/CT positive	15 (100%)
SUVmax average (range)	8.75 (4–14)
Lesion-to-liver SUVmax ratio average (range)	3.9 (1.8–6.7)
Lesion-to-blood pool SUVmax ratio average (range)	4.7 (3.6–7.7)

CRP, C-reactive protein; Pos, positive; FDG, fluorodesoxyglucose; SUV, standardized uptake value; N°, number; NR, normal range. * Low = less than the normal range values.

2.1. ^{18}F-FDG PET/CT Protocol and Interpretation

All ^{18}F-FDG PET/CT scans were performed after at least 6 h of fasting and with a glucose level lower than 150 mg/dL. A total of 3.5–4.5 MBq/Kg of ^{18}F-FDG activity was injected intravenously, and PET/CT scan was acquired 60 $\pm$ 10 min after the injection, from the base of the skull to the mid-thigh. PET/CT scanner used was a Discovery 690 tomograph (General Electric Company-GE-Milwaukee, WI, USA) with standard CT parameters (80 mA, 120 Kv without contrast; 4 min per bed—PET-step of 15 cm). The reconstruction was performed in a 256 $\times$ 256 matrix and field of view of 60 cm. A qualitative and a semiquantitative analysis of PET/CT images was performed by a reader (DA) with experience in this field; the maximum standardized uptake value (SUVmax), lesion-to-liver SUVmax ratio, and lesion-to-blood pool SUVmax ratio for the lesion with higher increased FDG uptake was calculated. SUVmax of the liver was calculated at the VIII hepatic segment using axial PET images with a round-shape region of interest (ROI) of 10 mm of diameter; instead, SUVmax of the blood-pool was measured at the aortic arch, avoiding the vessel wall by using a similar procedure. For qualitative evaluation, every focal FDG uptake different from physiological activity and background was considered as positive and potentially suggestive of disease. To evaluate treatment response after Rituximab, in absence of defined and shared criteria for MCD, we proposed the Deauville 5-point scale, such as for FDG-avid lymphoma [12,13]. With respect to the Deauville Criteria, ^{18}F-FDG PET/CT scans were considered negative for scores 1 to 3 and positive for scores 4 to 5.

2.2. Conventional Imaging

Patients were evaluated also by other conventional imaging (CI) studies, such as thoracic-abdominal CT. In all, the patients underwent 44 thoracic-abdominal CT: 15 for initial diagnosis, 11 for treatment response evaluation, and 18 for restaging/follow up. The interval between ^{18}F-FDG PET/CT scans and CT were within one week (range 1–7 days). For the evaluation of accuracy of restaging ^{18}F-FDG PET/CT, a combination of clinical and imaging follow-up (CT and/or subsequent PET/CT) for at least 12 months after ^{18}F-FDG PET/CT and/or histopathology (when available) was taken as reference standard. Because the histological verification of all lesions suspected for relapse identified at ^{18}F-FDG PET/CT was not clinically and ethically viable, the histopathology confirmation was available for seven cases. Lesions demonstrating increase in size on radiologic follow-up examinations and/or increase in ^{18}F-FDG uptake on subsequent PET/CT were considered as true positive and as lesions that demonstrated response after specific therapy on subsequent examinations.

2.3. Statistical Analysis

All statistical analysis was carried out using MedCalc (IBM, Chicago, IL, USA). The descriptive analysis of categorical variables comprised the calculation of simple and relative frequencies. The numeric variables were described as mean, minimum, and maximum. The relationship between semi-quantitatively features (SUVmax, lesion-to-liver SUVmax ratio, and lesion-to-blood pool SUVmax ratio) and the clinicopathological parameters were calculated using Kruskal–Wallis test and Mann–Whitney U test. Variables for which p-value < 0.05 in univariate analysis were subjected to multiple linear regression analysis to determinate those that were independently associated with semi-quantitatively features.

3. Results

3.1. ^{18}F-FDG PET/CT Baseline Findings

Among 15 ^{18}F-FDG PET/CT scans performed for diagnostic/staging purposes before any treatment, all resulted positive, showing the presence of several lymph nodes with increased FDG uptake, confirming the MCD diagnosis. In 11 cases, the FDG-positive lymph nodes were present at both sides of the diaphragm, while in the other four, they were only above diaphragm (Figure 1). The mean SUVmax of the ^{18}F-FDG avid lesions were 8.75 ± 3.1 (range 4–14), mean lesion-to-liver SUVmax ratio 3.9 ± 2.4 (range 1.8–6.7), and mean lesion-to-blood pool SUVmax ratio 4.7 ± 3.9 (range 3.6–7.7). No significant correlation was found between semiquantitative PET/CT parameters (SUVmax, lesion-to-liver SUVmax ratio, and lesion-to-blood pool SUVmax ratio) and gender, age, size, laboratory analyses, HIV status, and histologic subtypes. Instead, the presence of fever and the level of CRP were significantly correlated with SUVmax and SUVmax ratios values (Table 2). In fact, patients with fever and with high CRP levels had significantly higher SUVmax and SUV ratios values both at univariate and multivariate analysis.

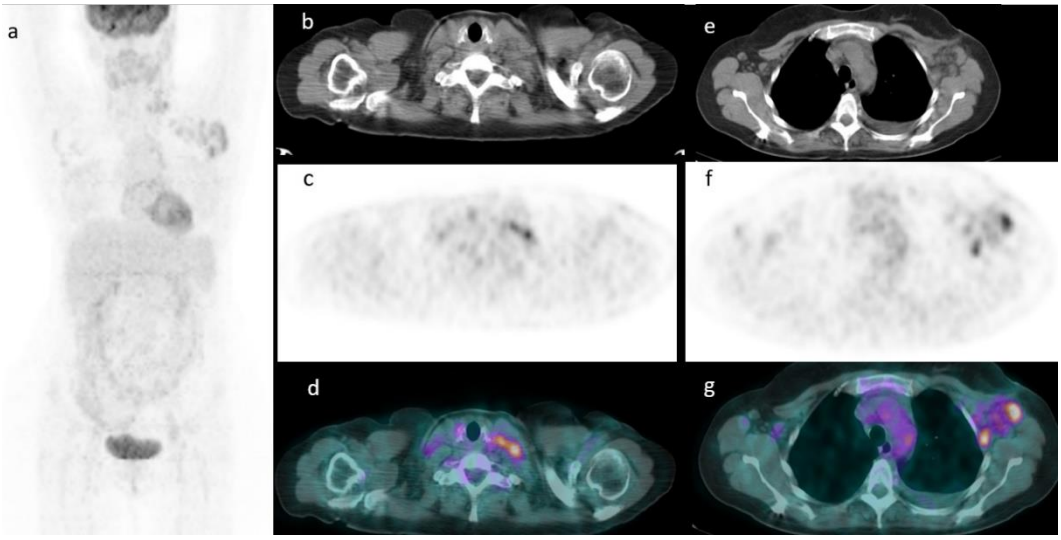

Figure 1. An example of a patients with FDG-avid laterocervical and axillary nodes at maximum intensity projection (MIP) (**a**). Axial CT (**b**), PET (**c**), and PET/CT fused images (**d**) confirming the presence of lymph nodes in left-side neck and in the left axilla (**e**–**g**).

Table 2. Comparison between SUVmax, lesion-to-liver SUVmax ratio, lesion-to-blood pool SUVmax ratio, and the main clinical-pathological features.

	aSUVmax	*p* Value	aL-L S Ratio	*p* Value	aL-B S Ratio	*p* Value
Age		0.222		0.356		0.310
Gender		0.884		0.501		0.941
Male	8.25		3.49		4.68	
Female	8.90		4.27		4.78	
Size		0.250		0.299		0.350
Fever		0.011 (0.024) *		0.028 (0.045) *		0.041 (0.049) *
Histologic subtype:		0.758		0.898		0.789
Hyaline Vascular	8.45		3.8		4.6	
Plasma cell	9.1		4		4.9	
Mixed	7.9		3.6		3.8	
Hemoglobin low (NR 130–180 man; 115–160 woman) (g/L)		0.333		0.252		0.352
Platelet low 10^9/l (NR 150–450)		0.210		0.222		0.422
Albumin low (g/L) (NR 4–5.4)		0.158		0.365		0.369
Leucocyte count low (NR 4–11) 10^9/L		0.625		0.700		0.600
CRP > 0.4 mg/L		0.001 (0.003) *		0.007 (0.012)		0.015 (0.041) *
LDH > 115 IU/L		0.258		0.301		0.500
HIV		0.308		0.464		0.441
positive	6.25		3.12		3.67	
negative	9.37		4.17		5	

aSUVmax, average SUVmax; aL-L S ratio, average lesion to liver SUVmax ratio; aL-B S ratio, average lesion to blood pool SUVmax ratio; NR, normal range. * between parenthesis *p* value of multivariate analysis.

3.2. Restaging/Follow Up ^{18}F-FDG PET/CT and Comparison with Other Imaging Modalities

Among the 15 patients for whom PET/CT was performed after the first-line therapy to evaluate treatment response, 7 (47%) showed the disappearance of any increased FDG uptake or the presence of faint uptake lower than mediastinum activity (Deauville score 1 in three cases, Deauville score 2 in four cases) (Figure 2), while the remaining 8 (53%) had a positive PET/CT displaying the persistence of at least one hypermetabolic lesion consistent with disease persistence (Deauville score 4 in five cases, Deauville score 5 in three cases). All patients with negative PET/CT after first-line therapy had no relapse of disease during the follow-up. Instead, of eight patients with positive PET/CT, only three reached a complete metabolic response during the course of disease. These patients received new treatment based on Rituximab in six cases and with Siltuximab in the other two. The other 22 PET/CT scans in 13 patients were performed during the follow-up, resulting negative in 17 cases and positive in 5 patients (Figure 3). In these five patients, a metabolic progression of disease was noted in four cases and an appearance of a new lesion consistent of relapse in the remaining case. Looking at all 22 restaging PET/CT studies, CI and restaging PET/CT were concordant in 14 patients (11 negative and 3 positive) and discordant in 8 (6 negative and 2 positive). Among concordant positive cases, both PET/CT and CI demonstrated the presence of pathological lymph nodes on the both sides of the diaphragm.

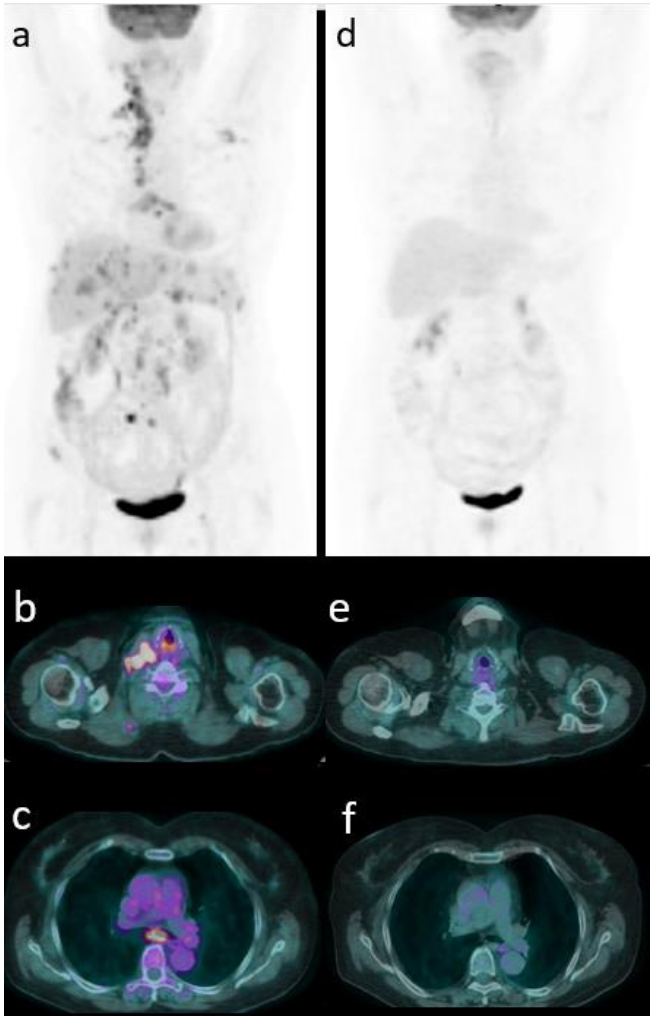

Figure 2. Baseline ^{18}F-FDG PET/CT (**a**) in a MCD patient with multiple lymph nodes above and below diaphragm with increased FDG uptake, such as in the right neck (**b**) and in sub-carena (**c**). PET/CT after 4 cycles of Rituximab showing a complete metabolic response (**d**) with the disappearance of the previous pathological lymph nodes (**e**,**f**) (Deauville score 1).

Analyzing discordant reports instead, ^{18}F-FDG PET/CT results compared to CT showed a complete metabolic response despite CT assessing enlarged lymph nodes suspected for persistence of disease in six cases, whereas it demonstrated a progression of disease (the appearance of new nodal and extranodal lesions) in presence of increased FDG uptake with concomitant stable disease at CT in two cases.

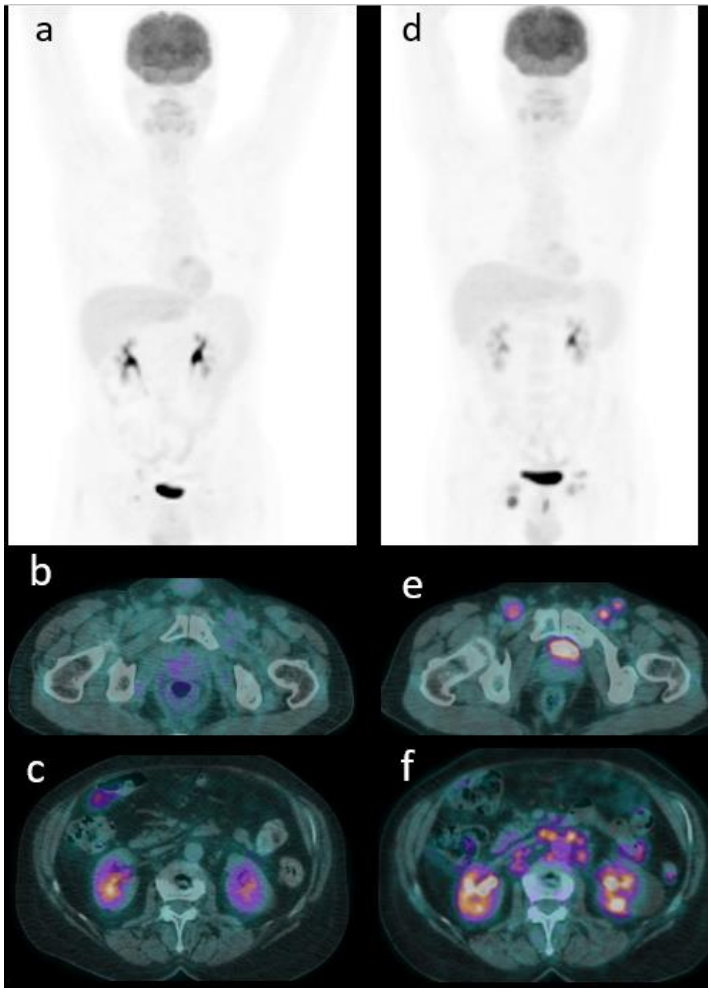

Figure 3. Restaging ^{18}F-FDG PET/CT (**a**) in a patient with moderate FDG uptake corresponding to right inguinal nodes (**b**,**c**). A follow-up PET/CT (**d**) demonstrating the metabolic progression of disease to the inguinal (**e**) and abdominal nodes (**f**).

4. Discussion

CD is a rare, lymphoproliferative disease potentially mimicking lymphoma or other diseases, like retroperitoneal paraganglioma [10]. The pathophysiology of CD is not fully clear, but it is well known that an inflammatory condition characterizes this disease, and this inflammation is directly related to interleukin 6 expression [14]. As in other inflammatory conditions [15], ^{18}F-FDG radiotracer may be accumulated in lymph nodes present in CD. Detection of involved lesions in CD is important for the determination of disease extension and multicentricity also due to the fact that, rarely, CD may evolve to lymphoma or multiorgan failure. However, in most cases, CD remains as a benign disease without complications or need of specific therapies. In the diagnostic field, the evidence of increased FDG uptake corresponding to lymph nodes may help to recognize CD patients with active and aggressive disease, as showed in our study. Among the 15 patients included, all had a positive PET/CT with multiple ^{18}F-FDG-avid lymph nodes. ^{18}F-FDG PET/CT demonstrated to be more accurate than CT in studying nodal involvement [8,9]: CT criteria are based on size and contrast enhancement. The presence of enlarged nodes with strong contrast enhancement is considered the diagnostic criterion for CD diagnosis despite the morphological features not always reflecting the disease status. Moreover, using this criterion lymph node without significant enlargement may be missed on CT.

Polizzotto et al. [16] studied 27 patients affected by Kaposi's sarcoma herpesvirus-associated MCD who performed ^{18}F-FDG PET/CT and demonstrated increased FDG uptake corresponding to lymph nodes, spleen, bone marrow, and salivary glands. Additionally, in our study, we showed increased FDG uptake to lymph nodes in all baseline PET studies and correlated with symptoms and CRP level. The metabolic activity of nodal disease is also similar with this study [16], with an average SUVmax of 8.7 (range 4–14) in our patients compared to 6 (range 2–8). However, Polizzotto et al. [16] included Kaposi's sarcoma herpesvirus-associated MCD, while in our study, only HHV8-associated MCD were recruited. Moreover, for the first time, to evaluate treatment response, we applied Deauville score and not only qualitative criteria.

Another potential advantage of ^{18}F-FDG PET/CT could be in the identification of the most suitable site for biopsy examination, which can help the correct diagnosis; however, strong evidences about this point are lacking and would need prospective studies. The metabolic behavior of MCD was very variable, as SUVmax ranges from to 4 to 14 and an average value of 8.75. PET/CT uptake (expressed as SUVmax, lesion to liver SUVmax ratio, and lesion to blood pool SUVmax ratio) were significantly higher in symptomatic patients (with fever) with high CRP level, underlying a possible relationship between metabolic aggressiveness and clinical conditions. Instead, the other laboratory findings (hemoglobin, platelets, LDH, albumin) were not related with PET/CT findings.

Another point evaluated by our work is the application of Deauville criteria to evaluate treatment response in MCD. Usually, the most common therapy of MCD consists of four cycles of Rituximab, but the response rate is very variable, and the risk of relapse is relatively high. The Deauville scale is a visual-qualitative score based on the comparison of residual uptake with target organs (liver and mediastinum), and it is commonly used in lymphoproliferative disease with high accuracy [12,13]. Nowadays, no previous studies have evaluated this scale in MCD setting. Thus, the real usefulness is yet unclear, but our evidences suggest a potential utility in this field. In fact, seven patients presented a negative PET after therapy with a Deauville score under 3, and these patients had no relapse during the subsequent follow-up. The aim to investigate the Deauville scores as a treatment response marker is due to the intrinsic limitation of CT in discriminating between fibrotic conditions and residual active disease [6], making this tool not ideal for MCD. The limitation of CT was also shown during the follow-up. The subsequent PET/CT scans revealed recurrences in five cases, while CT only in three, missing two patients where the size of nodes was stable. Besides, in six cases, CT suggested a possible progression of disease relapse due to the increase of node size or enhancement but without a corresponding radiotracer uptake increase and subsequent radiological examinations confirming the false negative findings of CT. These results underline the necessity of both-side information to predict disease status in MCD based on a combination of morphological (CT) and metabolic data (PET).

This work presents several limitations, such as the retrospective design of the study, the low number of patients included, and also due to the rarity of CD and the heterogeneity of patient's management (for example, not all patients attended all imaging examinations). It would be desirable to have further studies, possibly multicentric, to confirm or controvert these preliminary evidences.

5. Conclusions

In conclusion, we have demonstrated that ^{18}F-FDG PET/CT may be useful in evaluating patients affected by HHV-8-associated MCD both in the detection of active disease and in the evaluation of treatment response after Rituximab. Moreover, ^{18}F-FDG PET/CT seems to have a significant impact better than other conventional imaging methods during the follow-up.

Author Contributions: Conceptualization, D.A. and R.G.; methodology, F.B.; data curation, D.A. and F.D.; writing—original draft preparation, D.A., F.D. and F.B.; writing—review and editing, F.B. and R.G.; supervision, all. All authors have read and agreed to the published version of the manuscript.

Funding: This research received no external funding.

Institutional Review Board Statement: Ethical review and approval were waived for this study due to the retrospective design.

Informed Consent Statement: Informed consent was obtained from all subjects involved in the study.

Data Availability Statement: Not applicable.

Conflicts of Interest: The authors declare no conflict of interest.

References

1. Fajgenbaum, D.; Uldrick, T.S.; Bagg, A.; Frank, D.; Wu, D.; Srkalovic, G.; Simpson, D.; Liu, A.Y.; Menke, D.; Chandrakasan, S.; et al. International, evidence-based consensus diagnostic criteria for HHV-8-negative/idiopathic multicentric Castleman disease. *Blood* **2017**, *129*, 1646–1657. [CrossRef] [PubMed]
2. Jiang, J.P.; Shen, X.F.; Du, J.-F.; Guan, W.-X. A retrospective study of 34 patients with unicentric and multicentric Castleman's disease: Experience from a single institution. *Oncol. Lett.* **2018**, *15*, 2407–2412. [PubMed]
3. Oksenhendler, E.; Boutboul, D.; Fajgenbaum, D.; Mirouse, A.; Fieschi, C.; Malphettes, M.; Vercellino, L.; Meignin, V.; Gérard, L.; Galicier, L. The full spectrum of Castleman disease: 273 patients studied over 20 years. *Br. J. Haematol.* **2017**, *180*, 206–216. [CrossRef] [PubMed]
4. Fajgenbaum, D.C.; van Rhee, F.; Nabel, C.S. HHV-8-negative, idiopathic multicentric Castleman disease: Novel insights into biology, pathogenesis, and therapy. *Blood* **2014**, *123*, 2924–2933. [CrossRef] [PubMed]
5. Pria, A.D.; Pinato, D.; Roe, J.; Naresh, K.; Nelson, M.; Bower, M. Relapse of HHV8-positive multicentric Castleman disease following rituxi-mab-based therapy in HIV-positive patients. *Blood* **2017**, *129*, 2143–2147. [CrossRef] [PubMed]
6. Madan, R.; Chen, J.H.; Trotman-Dickenson, B.; Jacobson, F.; Hunsaker, A. The spectrum of Castleman's disease: Mimics, radiologic path-ologic correlation and role of imaging in patient management. *Eur. J. Radiol.* **2012**, *81*, 123–131. [CrossRef] [PubMed]
7. Koa, B.; Borja, A.J.; Aly, M.; Padmanabhan, S.; Tran, J.; Zhang, V.; Rojulpote, C.; Pierson, S.K.; Tamakloe, M.-A.; Khor, J.S.; et al. Emerging role of 18F-FDG PET/CT in Castleman disease: A review. *Insights Imaging* **2021**, *12*, 1–11. [CrossRef] [PubMed]
8. Barker, R.; Kazmi, F.; Stebbing, J.; Ngan, S.; Chinn, R.; Nelson, M.; O'Doherty, M.; Bower, M. FDG-PET/CT imaging in the management of HIV-associated multicentric Castleman's disease. *Eur. J. Nucl. Med. Mol. Imaging* **2008**, *36*, 648–652. [CrossRef] [PubMed]
9. Lee, E.S.; Paeng, J.C.; Park, C.M.; Chang, W.; Lee, W.W.; Kang, K.W.; Chung, J.-K.; Lee, D.S. Metabolic Characteristics of Castleman Disease on 18F-FDG PET in Relation to Clinical Implication. *Clin. Nucl. Med.* **2013**, *38*, 339–342. [CrossRef] [PubMed]
10. Jiang, Y.; Hou, G.; Zhu, Z.; Huo, L.; Li, F.; Cheng, W. The value of multiparameter 18F FDG PET/CT imaging in differentiating retro-peritoneal paragangliomas from unicentric Castleman disease. *Sci. Rep.* **2020**, *10*, 12887. [CrossRef] [PubMed]
11. Han, E.J.; Jung, S.E.; Park, G.; Choi, B.O.; Jeon, Y.W.; Min, G.J.; Cho, S.G. FDG PET/CT Findings of Castleman Disease Assessed by Histologic Subtypes and Compared with Laboratory Findings. *Diagnostics* **2020**, *10*, 998. [CrossRef] [PubMed]
12. Cheson, B.D.; Fisher, R.I.; Barrington, S.F.; Cavalli, F.; Schwartz, L.H.; Zucca, E.; Lister, T.A. Recommendations for initial evaluation, staging, and response as-sessment of Hodgkin and non-Hodgkin lymphoma: The Lugano classification. *J. Clin. Oncol.* **2014**, *32*, 3059–3068. [CrossRef] [PubMed]
13. Barrington, S.F.; Mikhaeel, N.G.; Kostakoglu, L.; Meignan, M.; Hutchings, M.; Müeller, S.P.; Schwartz, L.H.; Zucca, E.; Fisher, R.I.; Trotman, J.; et al. Role of Imaging in the Staging and Response Assessment of Lymphoma: Consensus of the International Conference on Malignant Lymphomas Imaging Working Group. *J. Clin. Oncol.* **2014**, *32*, 3048–3058. [CrossRef] [PubMed]
14. El-Osta, H.E.; Kurzrock, R. Castleman's Disease: From Basic Mechanisms to Molecular Therapeutics. *Oncologist* **2011**, *16*, 497–511. [CrossRef] [PubMed]
15. Vaidyanathan, S.; Patel, C.; Scarsbrook, A.; Chowdhury, F. FDG PET/CT in infection and inflammation—Current and emerging clinical applications. *Clin. Radiol.* **2015**, *70*, 787–800. [CrossRef] [PubMed]
16. Polizzotto, M.N.; Millo, C.; Uldrick, T.S.; Aleman, K.; Whatley, M.; Wyvill, K.M.; O'Mahony, D.; Marshall, V.; Whitby, D.; Maass-Moreno, R.; et al. 8F-fluorodeoxyglucose Positron Emission Tomography in Kaposi Sarcoma Herpesvirus–Associated Multicentric Castleman Disease: Correlation With Activity, Severity, Inflammatory and Virologic Parameters. *J. Infect. Dis.* **2015**, *212*, 1250–1260. [CrossRef] [PubMed]